The Journal of Neuroscience, March 1995, 15(3): 2240–2254

Several Types of Ca^{2+} Channels Mediate Glutamatergic Synaptic Responses to Activation of Single Thy-1–Immunolabeled Rat Retinal Ganglion Neurons

Holger Taschenberger and Rosemarie Grantyn

Developmental Neurobiology Group, Max Planck Institute for Psychiatry, 82152 Martinsried, Germany

A dissociated cell culture from the postnatal rat retina was established to characterize the synapses formed by retinal ganglion neurons (RGNs) *in vitro*. An antibody against Thy-1.1 was used to preselect putative RGNs for pair patch-clamp recording with the principal aim of identifying the released transmitter(s) and estimating the role of different types of voltage-activated Ca^{2+} channels in evoked transmitter release. The population of Thy-1+ neurons was heterogeneous. Staining patterns, soma-dendritic geometries and axon length displayed variations that could be related to basic electrophysiological properties, such as amplitudes of voltage-activated Na^+ currents ($I_{Na(V)}$), action potential size and capacity for repetitive discharge. Out of 73 coupled connections, 33 pairs were glutamatergic. With no exception, these connections were formed by the axons of strongly labeled Thy-1+ neurons with large $I_{Na(V)}$ (typically >2 nA) and repetitive firing over a broad current range. Such neurons were classified as RGNs. Forty out of 73 coupled pairs were GABAergic. These connections were always formed by weakly stained Thy-1+ neurons with small $I_{Na(V)}$ (typically <2 nA) and very limited capacity for repetitive discharge. Such neurons were tentatively classified as displaced amacrine cells. Evoked EPSCs in response to RGN activation were completely blocked by low concentrations of Cd^{2+} or Gd^{3+}. ω-CgTx-GVIA (5 μM) reduced EPSCs to 67 ± 29%, ω-AgaTx-IVA (200 nM) had no effect, and nifedipine (15 μM) enhanced the evoked EPSCs. Our experiments indicate that (1) the transmitter released by RGNs is glutamate and (2) the major part of synaptic glutamate release is governed by a novel toxin-resistant Ca^{2+} channel. The results further suggest that the characteristic phenotype of RGNs is well maintained in dissociated cell culture. In conjunction with electrophysiological tests Thy-1+ labeling can be used for RGN identification.

[Key words: retinal ganglion cell, Thy-1, synaptic transmission, glutamate, GABA, calcium channel]

Cat and rodent retinal ganglion neurons (RGNs) are among the well-characterized model neurons of the mammalian CNS. The spatial remoteness from their primary projection areas has been put to advantage in studies on pathway regeneration and map formation. However, the transmitter(s) of RGNs and the properties of synapses formed by these primary projection cells are still to be examined. We have now succeeded in maintaining putative RGNs in dissociated cell culture until they could form functional synaptic connections with other retinal neurons. This type of connection can be regarded as a physiological one, since intraretinal axon collaterals of ganglion cells were described for a variety of preparations (Dacey, 1985; Lau et al., 1992). In the present study, pair patch-clamp recordings were conducted to characterize presynaptic aspects of synaptic transmission between putative RGNs and other retinal neurons. Specifically, it was intended to provide unequivocal information on (1) the type(s) of transmitter(s) utilized by presumptive RGNs in their connections with other retinal neurons and (2) the type(s) of Ca^{2+} channels that govern transmitter release in these retinal synapses.

It is generally accepted that RGNs form excitatory connections, generate full size action potentials and produce spike trains if continuously depolarized. Available data point to glutamate (Glu) as a likely transmitter substance, at least in retinogeniculate (Crunelli et al., 1987; Sillito et al., 1990) and retinotectal (Sakurai et al., 1990; Roberts et al., 1991) connections. Apart from Glu, RGNs may contain substance P (Brecha et al., 1987) and other neuropeptides, including NAAG (Anderson et al., 1987). A minor fraction of RGNs stains for GABA or glutamate decarboxylase and is considered to be GABAergic (Yu et al., 1988; Caruso et al., 1989; Lugo-García and Blanco, 1991).

In contrast to the wealth of data on somatic Ca^{2+} currents, Ca^{2+} channels of axon terminals remained in general unexplored. Only exceptionally axon terminals are large enough to investigate their Ca^{2+} channels directly by electrophysiological methods (Stanley, 1993). In the CNS, one of the best characterized transmitter release systems is that of bipolar cells in the goldfish retina (Tachibana et al., 1993; Matthews et al., 1994). The giant terminals of these cells comprise only a single type (L) of Ca^{2+} channels which accounts for all the Glu release in synapses formed with amacrine cells and RGNs. In contrast, cerebellar climbing fibers (Regehr and Mintz, 1994) and the central terminals of DRG neurons (Yu et al., 1992) trigger Glu release under the control of two or more pharmacologically distinct types of Ca^{2+} channels, one of them being an N-type channel, as deduced from the block of synaptic transmission by ω-CgTx-GVIA. At least in case of the climbing fiber Purkinje cell syn-

Received May 19, 1994; revised Aug. 8, 1994; accepted Sept. 22, 1994.

We are indebted to the late Prof. H. D. Lux for critical reading of the manuscript. We thank H. Zucker, K. Gottmann, and F. Pfrieger for introduction into AutesP programming. The work was made possible due to a generous gift of brain derived neurotrophic factor by Amgen (Thousand Oaks). The technical assistance of Mrs. C. Pfitzner and Mrs. B. Jenke was excellent. This study has been supported by the Bundesministerium für Forschung und Technologie (Grant 16907A).

Correspondence should be addressed to Dr. Rosemarie Grantyn, Entwicklungsneurobiologie/BMFT, Max-Planck-Institut für Psychiatrie, Am Klopferspitz 18A, 82152 Martinsried, Germany.

apse, Glu is released via P-type Ca^{2+} channels which are specifically antagonized by low concentrations of ω-AgaTx-IVA. Thus, in different neurons release of the same transmitter could be controlled by a variety of Ca^{2+} channel types. This may provide diversity for the mechanisms of synaptic modulation and plasticity.

In freshly dissociated RGNs a larger part of the compound somatic Ca^{2+} current turned out to be resistant not only to dihydropyridines (DHPs), but also to the toxins ω-CgTx-GVIA and ω-AgaTx-IVA (Guenther et al., 1994). The present study will extend this observation by showing that these toxin-resistant channels control synaptic excitation elicited by single cell activation of identified retinal neurons in long-term cultures. The synapses formed by putative RGNs were always glutamatergic. Presumptive RGNs were preselected by vital immunolabeling with an antibody against the glycoprotein Thy-1.1, a commonly used procedure for identification of embryonic RGNs in dissociated cultures (Johnson et al., 1986; Barres et al., 1988; Rodríguez-Tébar et al., 1989). However, unlike the previously used approach of RGN selection according to size (Grantyn and Korenbaum, 1992; Guenther et al., 1994) or retrograde labeling (Karschin and Lipton, 1989) Thy-1 immunolabeling in long-term cultures is reliable only in conjunction with electrophysiological criteria.

A preliminary report has already appeared (Taschenberger and Grantyn, 1993).

Materials and Methods

Culture procedure. Our technique for preparation and maintenance of RGNs in long-term culture has already been briefly described (Rothe et al., 1994). For the present cultures we applied the following protocol. Postnatal Wistar rats were sacrificed at the age of P5. The retinas were dissected and stored in Ca^{2+}- and Mg^{2+}-free phosphate buffered saline. To ease the subsequent mechanical trituration retinal tissue was incubated for 30 min at 37°C in PBS containing 1 mM of cysteine-HCl and 15–20 U/ml papain. After this enzymatic treatment the tissue was dissociated in 0.05% DNase and 0.3% ovomucoid by passing it through a wide-bore Pasteur pipette. Cell suspensions were then centrifuged for 10 min at 500 rpm (45 × *g*). The supernatant was discarded, and cells were resuspended in growth medium (GM) supplemented with 2 ng/ml brain derived neurotrophic factor (BDNF, Amgen) and 2 ng/ml basic fibroblast growth factor (bFGF; Boehringer-Mannheim). Cells were seeded on laminin-coated ACLAR coverslips (Pro Plastics, Linden, NJ) at an initial density of 0.15–0.2 × 10^6 cells/cm^2. The GM consisted of MEM (GIBCO) with additions to reach the following final concentrations (in mM): L-glutamine 2, KCl 25, $NaHCO_3$ 25, HEPES 10, glucose 40, pyruvate 2. The GM was supplemented with 5% fetal calf serum and 5% horse serum (GIBCO), 27.5 μg/ml insulin (GIBCO), 2 ng/ml BDNF, 2 ng/ml bFGF and balanced to a pH of 7.4 with 5% CO_2. The GM was half-exchanged twice a week.

Immunostaining and visualization of RGNs. The coverslips bearing retinal cultures formed the bottom of a recording chamber that fitted into the movable stage of a Zeiss Axiovert 35 microscope. Freshly dissociated RGNs can be identified by retrograde labeling with the fluorescent dye Granular Blue (GB; Illing, Groβ-Umstadt) or other retrograde tracers. However, in our studies on synaptogenesis putative RGNs were selected by immunolabeling with an monoclonal antibody (mAb) against Thy-1.1 (clone MRC OX-7; Serotec). Anti Thy-1.1 was applied for 20 min at 37°C, at a dilution of 1:30 in standard salt solution (see below). The Thy-1 epitope was visualized by subsequent incubation with a phycoerythrin-conjugated goat anti-mouse F(ab')2 IgG fragment (Jackson Immuno Research Laboratories, 1:50) in bath solution. Phycoerythrin fluorescence was examined using the standard Zeiss filter set 015 (see Fig. 1 for appearance of unfixed cultures).

Cell counts. After the desired times *in vitro* cultures were fixed by application of 3% paraformaldehyde for 15 min at 4°C being either unstained (in case of retrograde labeling) or Thy-1 immunostained, as described above. In each experiment, entire coverslips were examined in duplicate. Labeled cells were counted and the counts were normalized to the number of labeled cells per cm^2 (Fig. 2). A rough estimate of neuron densities was obtained without additional staining solely based on cell geometries. Neuron densities were about 0.1 × 10^6/cm^2 on DIV 3–4 and 0.05 × 10^6/cm^2 on DIV 7–10. Higher initial seeding densities resulted in an increased number of dying neurons giving the same average neuron densities.

Recording conditions. For subsequent electrophysiological experiments the staining solutions were discarded and cultures were repeatedly washed with standard salt solution containing (in mM) NaCl 136, KCl 5, $MgCl_2$ 1, glucose 25, HEPES 15, $CaCl_2$ 5 (pH 7.3). The final osmolarity was adjusted to 370 mOsm/liter by adding sucrose. Culture dishes were placed on the stage of an inverted microscope (Axiovert 35, Zeiss) and the cells were viewed with phase-contrast or fluorescence optics. Individual cover slips were not used for more than 3 hr. All experiments were carried out at room temperature (22–24°C).

Ionic currents were recorded in the whole-cell configuration, using a conventional patch-clamp amplifier (List EPC-7). Currents were measured through a 500 MΩ feedback resistor and low-pass filtered at 3 kHz (three-pole Bessel filter). Capacitive transients were reduced by analog circuitry. Patch pipettes were pulled from thick-walled Duran glass (Schott Ruhrglas) on a Mecanex BB-CH micropipette puller (Mecanex SA, Switzerland). The DC resistances of patch electrodes ranged from 5 to 8 MΩ when filled with a solution of the following composition (in mM): K-gluconate 140, KCl 5, $CaCl_2$ 0.5, $MgCl_2$, EGTA 10, HEPES 25, glucose 10, ATP 2, cAMP 0.25, pH 7.3. The mean series resistance amounted to 11.6 ± 4.7 MΩ (range 6.7–25 MΩ, n = 35) and was compensated as much as possible (50–70%). In some cases (when recording voltage-activated Na^+ currents) high access resistances could result in serious voltage errors. However, these errors did not critically interfere with the results presented below.

Characteristics of voltage-activated Ca^{2+} currents were obtained from Thy-1–labeled (Thy-1+) neurons in short-term culture (between 4 and 48 hr *in vitro*) when labeled cells still bore few and short neurites (Fig. 1*A*). This provided relatively good space-clamp conditions. In order to isolate voltage-activated Ca^{2+} currents tetraethylammonium (TEA) was substituted for extracellular Na^+, and Ba^{2+} (10 mM) was used as charge carrier. Electrodes were filled with CsCl instead of K-gluconate to suppress voltage-activated K^+ currents. The holding voltage (V_h) was set to −90 mV. This prevented voltage-dependent inactivation of Ca^{2+} currents. Pulse frequencies did not exceed 1 per 15 sec to decrease current run-down.

Pair patch-clamp recording was carried out between DIV 6 and 14, when Thy-1+ neurons had already developed long processes that formed a dense network (Fig. 1*B,C*). At lower magnifications (100×) a Thy-1+ axon was easily distinguished by tracing it back from a position outside a cell's dendritic field. The axon was then examined at higher magnification (400×) for possible contact with other neurons in the same visual field. This strategy helped to preselect potentially coupled retinal neurons. Usually, a Thy-1+ neuron was picked first and then the second cell of the pair was found based on the presence of axonal contacts. This cell could either be Thy-1+ or Thy-1 negative. Both neurons were maintained for 10–30 min in a stable voltage-clamp configuration at V_h −65 mV. Synaptic responses could be induced when the presynaptic neuron was held either in the voltage-clamp or in the current-clamp mode. In both cases short depolarizing pulses were applied to the presynaptic Thy-1+ neuron at a frequency of no more than 1/5 sec. Usually, voltage clamp was preferred for the reason of higher stationarity of the release process. Due to the complex geometry of differentiated Thy-1+ neurons only somatic and proximal dendritic membrane compartments could be expected to be under full voltage control. Therefore short but strong depolarizations (pulses to somatic voltage levels between −20 and +20 mV) were used to elicit single presumably propagated spikes and transmitter release from the unclamped axon terminal.

Drug application. During the recording sessions, cells were kept under a continuous flow of standard or test solutions. Drugs were applied by a gravity-driven manually operated six-barrel superfusion system which allowed for rapid exchange of solutions (<500 msec). The superfusion pipette (tip diameter 50–100 μm) and the suction pipette (tip diameter 100–200 μm) were placed opposite to each other at a distance of about 150 μm to the selected cell. The suction pipette prevented a contamination of the bath solution outside the dendritic field of the postsynaptic cell (see Kraszewski and Grantyn, 1992, for detailed description of this microsuperfusion technique). Pharmacological analysis of voltage-activated Ca^{2+} currents was carried out using ω-conotoxin-

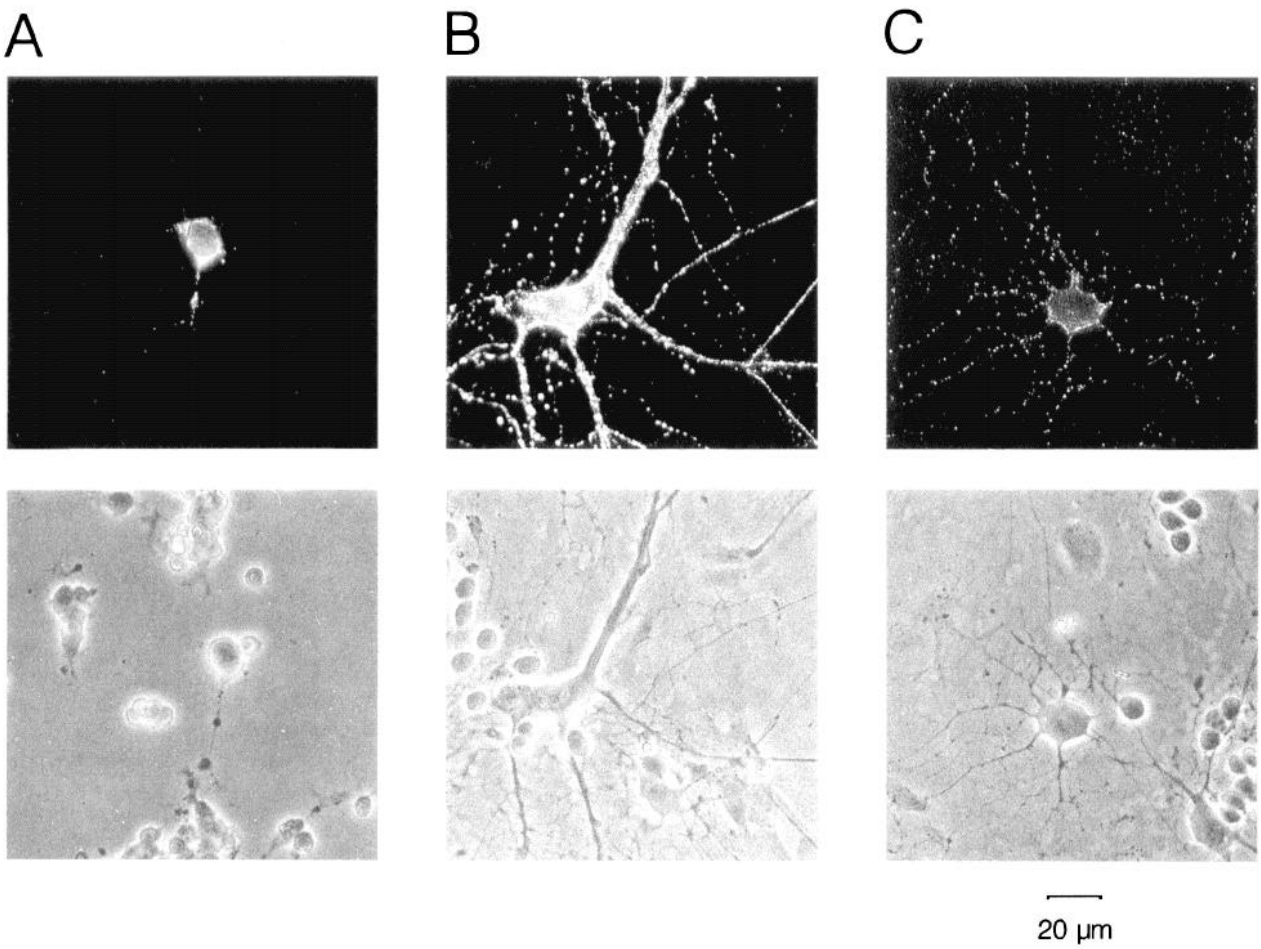

Figure 1. Fluorescent (*upper row*) and phase contrast images (*bottom row*) of Thy-1+ neurons in dissociated cultures from postnatal rat retinae. *A*, Freshly dissociated culture after 24 hr in culture. *B*, Example of bright Thy-1 labeling after 13 d *in vitro*, *C*, Example of weak Thy-1 labeling after 13 d *in vitro* from the same culture dish under same staining conditions as *B*. Note differences in dendritic geometry. Typically, in bright Thy-1+ neurons heavy stem dendrites come out at variable positions from an irregularly shaped soma. In weakly fluorescent Thy-1+ neurons very slim stem dendrites often extend in a radial starburst manner from a round soma.

GVIA (ω-CgTx-GVIA; Bachem, Heidelberg), ω-agatoxin-IVA (ω-AgaTx-IVA; Alomone Labs, Jerusalem), BAY K8644, nitrendipine, and nifedipine (Sigma). Nitrendipine was dissolved in DMSO. Nifedipine and BAY K8644 were dissolved in ethanol. Stock solutions were diluted to at least 1:1000. All DHP containing vessels were protected against light. 6,7-Dinitroquinoxaline-2,3-dione (DNQX) was purchased from Tocris Neuramin.

Data analysis. Voltage-activated currents and stimulus-evoked postsynaptic currents were digitized on-line by a labmaster DMA interface and pCLAMP software (Axon Instruments) at a sampling frequency of 8–20 kHz. Off-line analysis was performed using the AUTESP software by H. Zucker (Garching Instruments). Input resistance was estimated from the averaged steady state current at the end of small (10–20 mV) hyper- or depolarizing voltage steps at normal V_h. Kinetic parameters of synaptic currents were obtained by an automated routine in the AUTESP programming language. Rise times of postsynaptic currents were calculated as the time from 20 to 80% of the peak amplitude. The time course of decay was fitted by a single exponential. Accuracy of fitting procedures was checked by eye. Results are reported as mean ± SD. Statistical comparisons were made using the two-tailed Student's *t* test.

Results

Thy-1+ neurons are supported by BDNF and survive in dissociated cell cultures until synapses are formed

Antibodies against the membrane glycoprotein Thy-1 were used with the intention of RGN identification. Combining retrogradely transported GB and Thy-1 immunolabeling in the postnatal rat retina at P4–6 we found that nearly 90% of all neurons with soma size >8 μm were double labeled after multiple GB injections in the superior colliculus (Grantyn and Korenbaum, 1992). The remaining neurons were Thy-1+ only. Although a small number of unlabeled cells is to be expected in any retrograde tracer experiment serious doubts were repeatedly raised with regard to the selectivity of Thy-1 antibodies in the rodent retina in general (Perry et al., 1984; Barres et al., 1988), and retinal cultures in particular (Barres et al., 1988). In view of these objections we initially attempted to investigate synaptogenesis in retrogradely labeled RGNs essentially following the approach of Huettner and Baughman (1988) who studied corticotectal neurons. Although the survival rate of GB-labeled (GB+) RGNs in dissociated culture was reported to be rather low (Takahashi et al., 1991) we expected to obtain long-term survival by adding BDNF to the culture medium. This neurotrophin is known to support embryonic rat (Johnson et al., 1986) and chick (Rodríguez-Tébar et al., 1989) RGNs in culture.

However, despite the addition of 2–10 ng/ml of BDNF the number of GB+ neurons decreased rather fast within few days *in vitro* (Fig. 2). The low incidence of GB+ cells after 48 hr was not the result of tracer leakage or fainting, since double labeling with anti-Thy-1 revealed a similar rapid decrease of

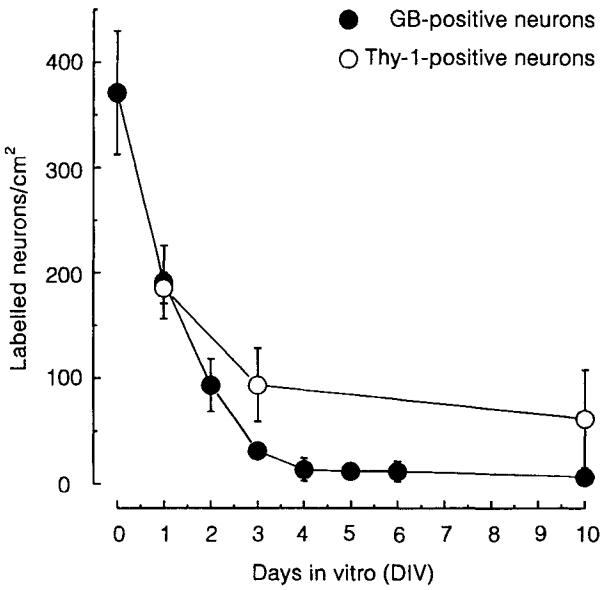

Figure 2. Survival rate of GB+ and Thy-1+ neurons during the first 10 d *in vitro*. Data points represent the mean ± SD from three experiments. The average number of GB+ neurons in the dish after 10 d was 11.4 when plated on a preformed astrocyte monolayer (see Grantyn and Korenbaum, 1992). The survival was less on laminin. A substantially higher number of putative RGNs was found with Thy-1 immunostaining. The average number of Thy-1+ neurons on laminin after 10 d was 62 ± 46 cells/cm². For both experiments recombinant BDNF from Amgen was applied at a concentration of 2 ng/ml. bFGF (Boehringer) and insulin (GIBCO) were added at a final concentration of 2 ng/ml and 32 μg/ml, respectively. All conditions were exactly as used for experiments on synaptic transmission.

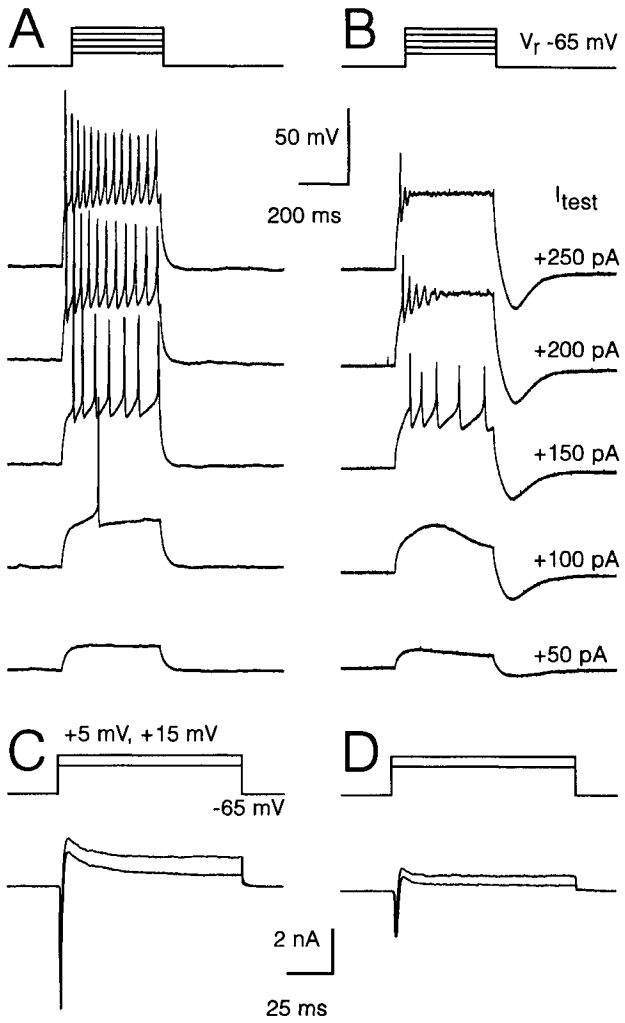

Figure 3. Firing behavior of two different Thy-1+ neurons after 2 weeks in culture. In each column, respectively: *top* (*A*, *B*), response to steady depolarization (current-clamp record); *bottom* (*C*, *D*), voltage-activated conductances (mixed $I_{Na(V)}$ and $I_{K(V)}$, voltage-clamp record). Amplitudes of injected currents are indicated on the right of each row. For *A–C*, resting potentials were adjusted to −65 mV by a small holding current. *A* and *C*, Records from a brightly labeled Thy-1+ neuron with sustained discharge over a wide range of injected current. *B* and *D*, Records from a weakly labeled Thy-1+ neuron that generated a sustained discharge only over a narrow current range. Note slow afterhyperpolarization in *B* but not *A*. *C* and *D*, Voltage-activated Na^+ and K^+ currents induced by voltage steps from −65 mV to +5 mV (*lower trace*) and to +15 mV (*upper trace*). Note that the weakly labeled Thy-1+ neuron (*D*) generated smaller $I_{Na(V)}$ and $I_{K(V)}$ than the strongly labeled Thy-1+ neurons of *D* and *E*. All records in 5 mM $[Ca^{2+}]_o$. Electrodes were filled with K-gluconate.

Thy-1+ neurons. We therefore returned to the method of vital immunostaining with the hope that electrophysiological experiments would provide additional criteria to complement Thy-1–based identification of RGNs. This approach proved to be successful. First of all, the number of surviving Thy-1+ neurons was more then sufficient to choose between several healthy candidates for patch-clamp experiments (Figs. 1*B*,*C*; 2). Second, electrophysiological experiments confirmed that RGNs could probably be selected not only according to their staining pattern, neuron morphology, but also according to the size of voltage-activated Na^+ currents and the repetitive firing behavior, that is, properties that are easy to investigate routinely (Fig. 3). Third, we succeeded in maintaining Thy-1+ neurons for the time necessary for synaptogenesis. This provided the additional option of confronting observations on basic morphological and electrophysiological properties of labeled neurons with the postsynaptic response to single cell activation (see Fig. 6). The minimal survival time required for this purpose was 4–6 d *in vitro*. While spontaneous synaptic activity appeared in a majority of cells already by DIV 4, the incidence of evoked synaptic responses was low until DIV 6.

Retinal neurons varied in their Thy-1 staining pattern

We can only underline the previous notion (Barres et al., 1988) that the mere existence of Thy-1+ neurons in retinal cultures cannot be regarded as sufficient evidence for survival of RGNs. Although astrocytes were not stained under the present growth conditions, there was always strong labeling of fibroblast-like cells. After one week *in vitro*, the latter could easily be recognized. Among the population of Thy-1+ neurons, one could distinguish two main cell types. The first group will be referred to as strongly labeled Thy-1+ neurons (Fig. 1*B*), whereas neurons of the second group will be qualified as weakly labeled Thy-1+ neurons (Fig. 1*C*). Neurons belonging to the first group displayed Thy-1 immunoreactivity in discontinuous very bright spots of more than punctuate size covering the entire cell, except the growth cones. In older cultures these cells were characterized by the presence of usually three or four heavy stem dendrites emerging from a multipolar soma with an eccentric nucleus (Fig. 1*B*). Although these cells were among the largest in culture, a size criterion could not be used after 48 hr *in vitro*, since some unlabeled somata were of equally large size and shape. The axon

Table 1. Characteristics of RGNs and putative displaced amacrine cells in culture (DIV 6–14)

	RGNs	Putative displaced amacrine cells	Significance of differences
Thy-1 staining	Strong	Weak	
Soma shape	Irregular	Round	
Stem dendrites	Heavy	Fine	
Axon length (μm)	>2500	<250	
Axon collaterals	Many	Few	
Yield of short distance coupling	Low	High	
Av. amplitude of AP (mV)	111	76	$p < 0.01$
Current-range of repetitive firing in response to steady depolarization (pA)	≥ 150	≤50	
Slow afterhyperpolarization	Not detected	Prominent	
Av. amplitude of $I_{Na(V)}$ (nA)[a]	4.62 (glutamatergic cells)	0.80 (GABAergic cells)	$p < 0.05$
Released transmitter	Glutamate	GABA	
Av. amplitude of PSC (pA)	198.9	528.4	$p < 0.01$
Av. time constant of PSC decay (msec)	1.97	36.3	$p < 0.001$
Av. PSC rise time (msec)	0.63	1.37	$p < 0.001$

[a] Data refer to the set of presynaptic cells with demonstrated transmitter phenotype as shown in Figure 6.

of strongly labeled Thy-1+ neurons could be recognized at lower magnification because it left the dendritic area of the mother cell to spread throughout the culture dish. As a rule, collaterals went off at an angle of about 90°. With some exercise it was quite possible to distinguish a Thy-1+ axon from a Thy-1+ dendrite according to their ramification patterns.

Weakly labeled Thy-1+ neurons were characterized by punctate immunostaining. Slim dendrites emerged from a usually rounded soma with a central nucleus (Fig. 1*C*). The dendritic field and total axon length was often smaller than in heavily labeled Thy-1+ neurons, although these properties overlapped to some extent. If no functional criteria were available to distinguish between strongly and weakly labeled Thy-1+ neurons it would perhaps not always be easy to qualify them as belonging to one or the other population. However, the structural properties mentioned above correlated with differences in functional parameters which, in turn, helped to sharpen the eye for the existing differences in the staining pattern (see Table 1 for more details).

Strongly and weakly labeled Thy-1+ neurons differ with regard to repetitive firing behavior and voltage-activated Na^+ currents

The repetitive firing behavior of any neuron reflects the interplay of several ion conductances. Differences in ion channel profiles should create differences in repetitive firing. In some structures peculiarities of repetitive firing behavior may therefore be regarded as functional markers and used for neuron identification (Grantyn et al., 1983). In the intact rodent retina only ganglion cells are expected to respond to prolonged depolarization with action potential trains, although some amacrine cells seem to have axons (Dacey, 1990), at least transiently (Hinds and Hinds, 1983), which possibly generate single action potentials (Gleason et al., 1993). We compared the firing behavior of strongly and weakly labeled Thy-1+ neurons (Fig. 3). In the current-clamp mode, depolarizing pulses of different amplitude were applied to a total of 34 Thy-1+ neurons. It was found that every Thy-1+ neuron generated at least one action potential (AP) in response to appropriate steady depolarization. In strongly labeled Thy-1+ neurons the firing was continuous throughout a period of 1000 msec and more (Figs. 3*A*, 4). At higher current intensities APs tended to inactivate, as indicated by their broadening and amplitude decrease. Maximal frequencies of steady state firing ranged from 15 to about 35 imp/sec (Fig. 4). These values should, however, be taken with some caution. After *in vivo* development maximal frequencies of RGNs could occasionally reach 70 imp/sec. The present values are in agreement with observations on visually stimulated mice RGNs (Balkema and Pinto, 1982; Stone and Pinto, 1993), but are much below the frequencies of cat RGNs under noninvasive recording conditions (Kuffler, 1953; Lankheet et al., 1989).

In the present context it is important to note that the current range of continuous repetitive firing was always much broader in strongly labeled Thy-1+ neurons (150 pA) as compared to weakly labeled Thy-1+ neurons (50 pA) (compare Figs. 3*A* and 4 with Fig. 3*B*). In the latter group, many cells never generated more than one AP. There was no difference in the mean values of resting membrane potentials between strongly and weakly labeled Thy-1+ neurons. In general, membrane potentials varied between −32 and −69 mV, (mean −53.0 ±7.6 mV, $n = 116$), when measured immediately after achievement of the whole-cell configuration.

The amplitude of evoked action potentials were different in strongly labeled Thy-1+ neurons with repetitive firing, as compared to weakly labeled Thy-1+ neurons without repetitive firing. The respective values were 111 ±16 mV ($n = 20$) and 76 ±17 mV ($n = 8$). The difference was significant at $p < 0.01$.

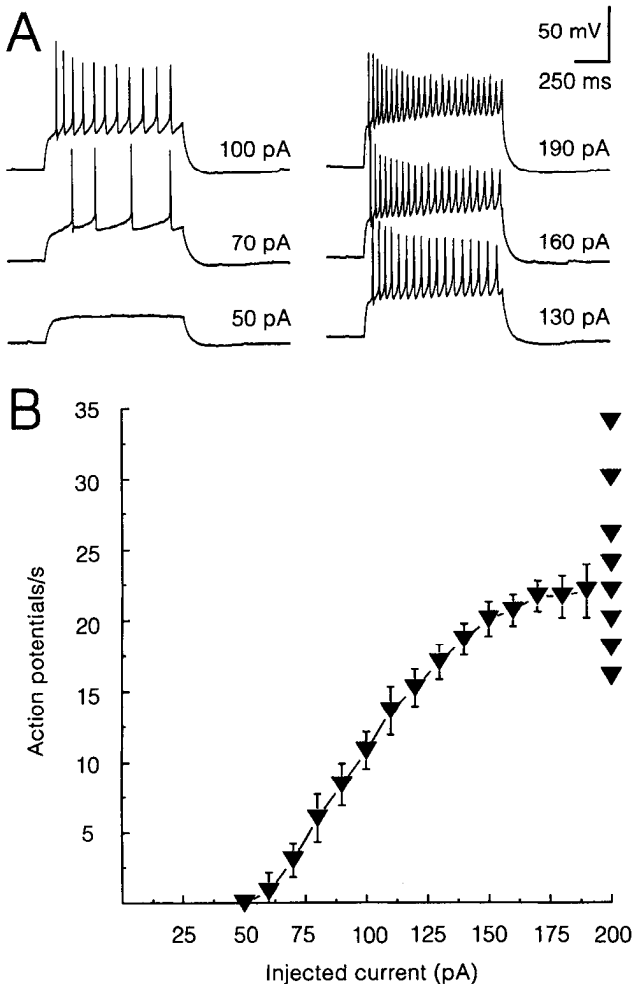

Figure 4. Voltage response of putative RGNs to injection of current steps (magnitude shown at each trace). *A*, Strongly labeled Thy-1+ neuron generating repetitive trains of APs. At larger injected current the APs tended to decrease in their amplitudes. *B*, Frequency–current characteristics from the cell shown in *A* (average from four trials). Note the linear dependence of discharge frequency on injected current between 50 and 190 pA. *Triangles on the right* indicate levels of discharge frequency in eight different RGNs following a depolarizing current pulse of 200 pA.

Among the features that clearly separated strongly labeled from weakly labeled Thy-1+ neurons was not only the size of voltage overshoots during the APs but also the presence of slow afterhyperpolarizations following the depolarizing current pulse (compare Fig. 3*A,B*). Finally, in both sets of neurons substantial differences were found in the amplitudes of voltage-activated Na^+ currents ($I_{Na(V)}$) (compare Fig. 3*C,D*, and see Fig. 6), the values being 7.02 ± 3.12 nA (range, 3.0–15.5 nA) and 0.98 ± 0.78 nA (range, 0.3–2.5 nA), for strongly and weakly Thy-1+ cells, respectively. Thy-1+ neurons that lacked $I_{Na(V)}$ were never found (109 cells tested). In contrast, within the population of multipolar Thy-1–negative neurons some cells were apparently unable to generate TTX-sensitive $I_{Na(V)}$. Six out of 34 neurons could not be allocated into any of these two groups, since the cells produced large APs and lacked a slow AHP, but failed to generate repetitive trains of APs.

Taken together, these results confirm a previous notion (Barres et al., 1988) that frequency–current relationships and $I_{Na(V)}$ could serve to distinguish between putative RGNs and other Thy-1+ neurons in culture. We regard strongly labeled Thy-1+ neurons with amplitudes of $I_{Na(V)}$ >2 nA, a broad repetitive firing range and absence of a slow AHP as RGNs. Weakly labeled Thy-1+ neurons with $I_{Na(V)}$ typically <2 nA, a narrow repetitive firing range and prominent slow AHP will be referred to as putative displaced amacrine cells.

Only RGNs form glutamatergic synapses with other retinal neurons in culture

Figure 5 depicts typical soma-dendritic profiles and experimental arrangements used to test for synaptic coupling of Thy-1+ cells with other neurons in culture. The present material was obtained from a total of 73 coupled pairs. Nine synaptic connections were formed with another Thy-1+ neuron (Fig. 5*A*). Sixty-four connections were built between a Thy-1+ and a Thy-1–negative neuron (Fig. 5*B,C*). In many cases the connections were reciprocal. We were, however, only interested in synaptic connections formed by identified axons and therefore discarded pairs with unlabeled neurons contacting Thy-1+ neurons.

The most surprising finding was that Thy-1+ neurons could assemble either glutamatergic (33/73 pairs; Fig. 5*B*) or GABAergic (40/73 pairs; Fig. 5*C*) synaptic connections, as deduced from the contrasting time course of postsynaptic currents (compare Fig. 5*B,C*) and the complete block of synaptic responses by either DNQX (Fig. 7*C*) or bicuculline methiodide (Fig. 8*C*). At any time *in vitro* there was a strict coincidence between the type of transmitter released and the class of Thy-1+ neurons as defined in terms of RGN versus displaced amacrine cells. Glu releasing cells were always strongly Thy-1+ labeled neurons with large $I_{Na(V)}$ (4.62 ± 2.67 nA; range, 1.22–12.23 nA) and continuous firing capacity (Figs. 6*C*, 7*A*; Table 1). In contrast, GABA-releasing cells were always weakly Thy-1+ labeled. They generated smaller $I_{Na(V)}$ (0.80 ±0.50 nA; range, 0.30–2.04 nA), single spikes and slow AHPs after prolonged depolarizations (Figs. 6*C*, 8*A*; Table 1).

Figure 6 illustrates the correlation between the type of Thy-1+ neuron, as defined on the basis of $I_{Na(V)}$, and the type of released transmitter, as identified in the pair recording paradigm. $I_{Na(V)}$ was estimated as the peak inward current from a family of current traces evoked by depolarizing voltage steps to different membrane potentials (between −45 and 45 mV, V_h −65 mV). For Thy-1+ neurons with demonstrated coupling the data points were represented by a special symbol. At least from DIV 10 on the differences in $I_{Na(V)}$ between glutamatergic and GABAergic Thy-1+ neurons were obvious. The respective average values were for glutamatergic Thy-1+ neurons 4.62 nA (±2.67 nA, range 1.22–12.23 nA, n = 21) and 0.80 pA for GABAergic Thy-1+ neurons (±0.50 nA, range 0.30–2.04 nA, n = 11).

The results of Figure 6*C* may be biased in two ways. First, although strongly labeled RGNs neurons were more abundant at any age, it turned out to be difficult to find their postsynaptic partner within the same field of observation. The axons of these cells tended to contact neurons at large distance (Table 1). In contrast, weakly labeled Thy-1+ neurons were less frequently encountered, but it was relatively easy to elicit synaptic responses in neighboring cells. Second, it is not excluded that Thy-1 labeling of weakly stained cells was better resolved in older cultures. However, no obvious sequence was found in the expression of the glutamatergic versus the GABAergic Thy-1+ phenotype.

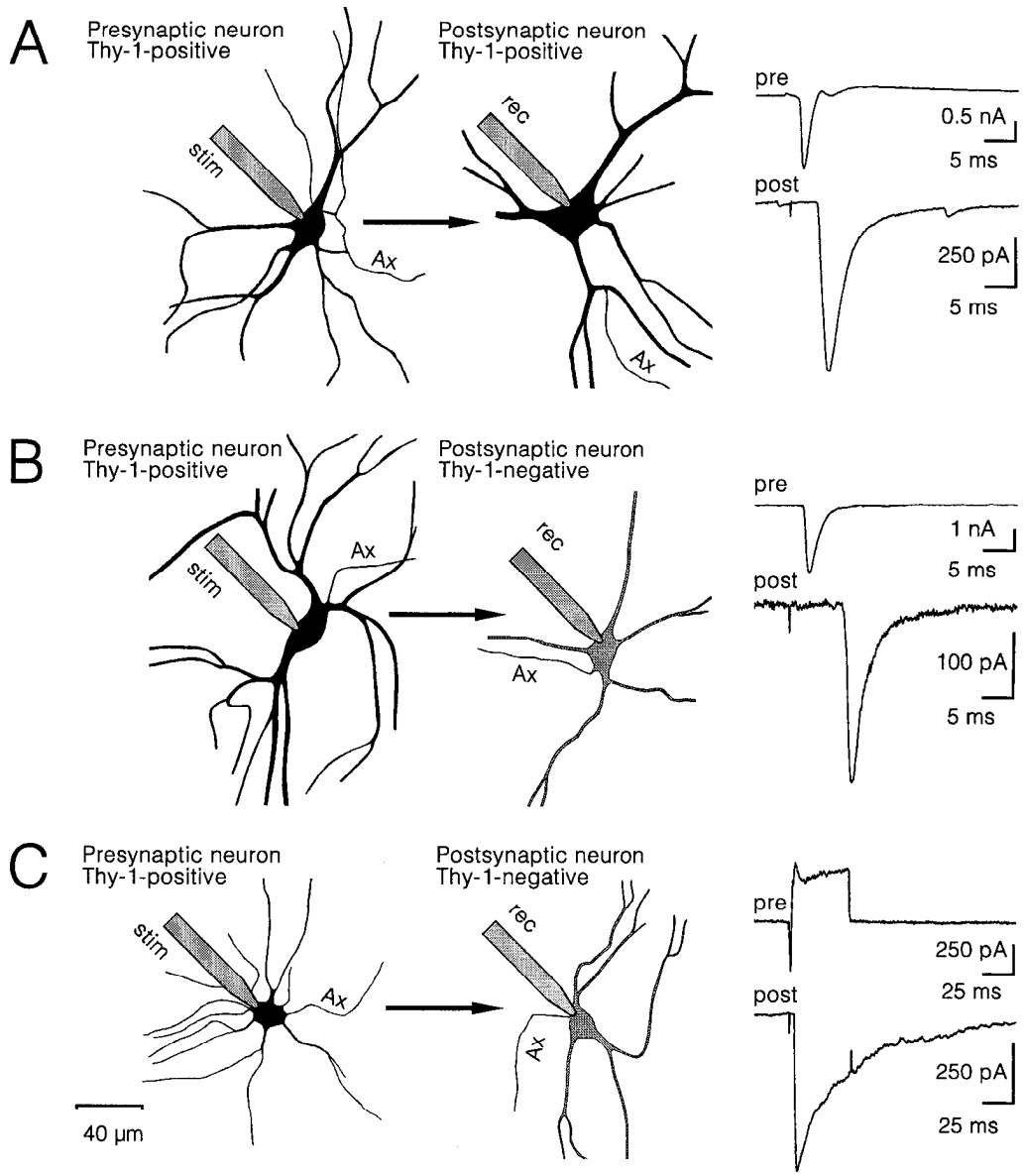

Figure 5. Experimental arrangement for pair patch-clamp recording to investigate transmitter release properties of presynaptic Thy-1+ neurons. Postsynaptic neurons were either Thy-1+ neurons (*A*) or Thy-1-negative neurons (*B, C*). Presynaptic neurons were either strongly Thy-1–immunolabeled RGNs (*A, B*) or weakly Thy-1–immunolabeled neurons (*C*). *Right column*, typical examples of $I_{Na(V)}$ in presynaptic cells (*upper traces*) and postsynaptic responses (*lower trace*). *A*, EPSC induced in a Thy-1+ neuron by presynaptic depolarization to −15 mV of a Thy-1+ neuron. Record on DIV 14. *B*, EPSC recorded from a Thy-1–negative neuron on DIV 19. *C*, Depolarization of a weakly labeled Thy-1+ neuron to +15 mV evoked IPSCs in a Thy-1–negative neuron (DIV 13). Note the difference in time scale and depolarization required for activation of synaptic response in *C*. The soma-dendritic profiles were traced from photomicrographs. The neurites designated with *Ax* were the axons.

Basic properties of glutamatergic and GABAergic synapses formed by Thy-1+ neurons in vitro

Figure 7 illustrates a standard experiment to characterize glutamatergic synaptic transmission between RGNs and other retinal neurons. It can be seen that glutamatergic synaptic transmission depended on the generation of presynaptic $I_{Na(V)}$, since application of 1 µM TTX completely and reversibly blocked the postsynaptic response (Fig. 7*B*). Activation of release sites by direct depolarization in the presence of TTX was never obtained. The postsynaptic response was completely and reversibly blocked by the competitive AMPA/kainate receptor antagonist DNQX (Fig. 7*C*), thus demonstrating the glutamatergic nature of the activated synapse. Under conditions of blocked voltage-activated K^+-currents (CsCl-filled electrodes) the EPSCs could be reversed by variation of the membrane potential (Fig. 7*D,E*). Current–voltage relationships were linear (Fig. 7*E*). This result indicates that most activated terminals on the postsynaptic cell were located at close electrotonic distance to the somatic recording electrode because the driving force for the excitatory synaptic current was fully controlled. EPSCs had a mean amplitude of 198.9 ± 182.3 pA (n = 33), a mean rise time of 0.63 ± 0.17 msec (n = 33) and a mean time constant of decay (t_D) of 1.97 ± 0.62 msec (n = 31).

It should be pointed out that the EPSCs recorded here are among the shortest EPSCs ever measured (see Schneggenburger et al., 1992, for references). Our records were usually taken in the presence of 1 mM Mg^{2+} and at V_h of −65 mV. This largely excluded a contribution of NMDA receptors to the synaptic re-

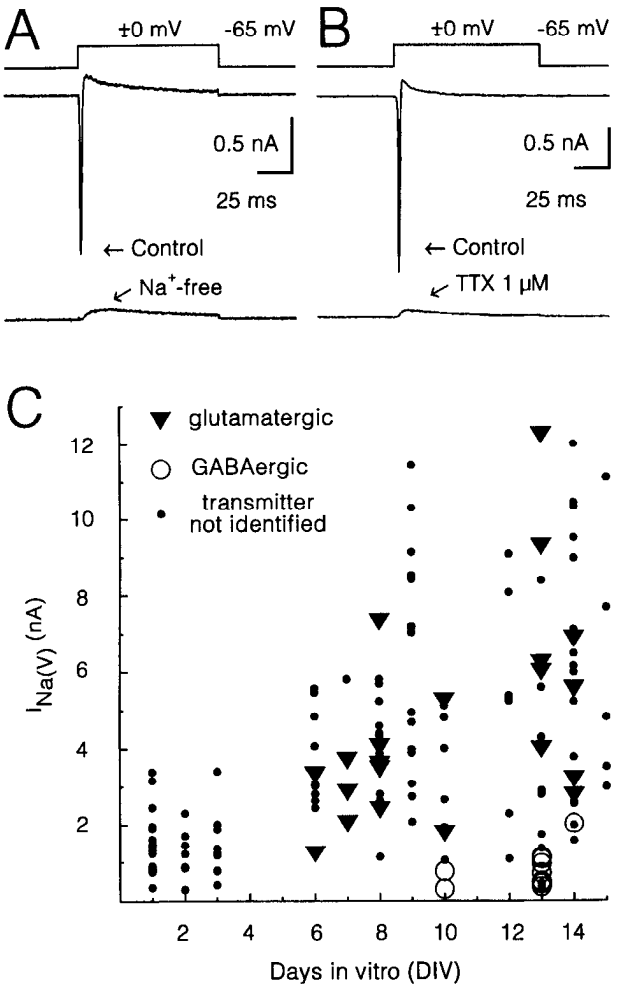

Figure 6. Relationship between types of released transmitter and amplitudes of $I_{Na(V)}$ at different times *in vitro*. *A* and *B*, Records illustrating identification of $I_{Na(V)}$ in two RGNs. *C*, Plot of $I_{Na(V)}$ amplitudes of Thy-1+ neurons against time *in vitro*. *Solid triangles*, data points from heavily stained Thy-1+ neurons with the characteristics of RGNs. These neurons gave rise to glutamatergic EPSCs. *Open circles*, data points from weakly labeled Thy-1+ neurons that gave rise to GABAergic IPSCs. *Small dots*, data points from Thy-1+ neurons without established transmitter phenotype. During the 2nd week *in vitro* differences of $I_{Na(V)}$ in glutamatergic and GABAergic neurons were significant (*t* test, $p < 0.05$). It can also be seen that in glutamatergic neurons increase of $I_{Na(V)}$ proceeded throughout the period of investigation. In contrast, $I_{Na(V)}$ of GABAergic cells remained on the same low level throughout the 2nd week *in vitro*.

sponses elicited by putative RGNs. To clarify a possible role of NMDA receptors we omitted Mg^{2+} from extracellular solutions, varied V_h and tested the blocking action of APV. However, in none of the cases (five pairs) a longer-lasting or DNQX-resistant component appeared. Thus, under the given experimental conditions a participation of NMDA receptors was not detectable, although responses to exogenous NMDA were observed in many retinal neurons. Six out of 13 Thy-1+ neurons generated NMDA-activated currents in the absence of Mg^{2+} and in the presence of 1 µM glycine. Amplitudes of NMDA-activated currents were, on average 49 ± 27.1 pA ($n = 6$). More details on the postsynaptic properties of glutamatergic synapses between retinal neurons will be given elsewhere.

The properties of GABAergic synaptic transmission following activation of putative displaced amacrine neurons are illustrated in Figure 8. The responses were completely and reversibly blocked by TTX (Fig. 8*B*) and bicuculline methiodide (Fig. 8*C*). IPSCs reversed at 0 mV when using symmetrical Cl^- concentrations (Fig. 8*D,E*) and at more negative holding potentials (−30 to −50 mV) when using K-gluconate (not illustrated). IPSCs displayed linear current–voltage relationships (Fig. 8*E*) and had a mean amplitude of 528.4 ± 674.9 pA ($n = 37$) and a mean rise time of 1.37 ± 0.40 msec ($n = 34$). The mean t_D value was 36.3 ± 9.4 msec ($n = 38$). Thus, as in other structures, GABAergic synapses were distinguished from glutamatergic synapses on the basis of their slower time course.

A major component of glutamate and GABA release from Thy-1+ neurons is resistant to the available channel-selective Ca^{2+} current blockers

In order to clarify which types of voltage-activated Ca^{2+} channels may govern transmitter release in RGNs we tested the action of several channel-selective blockers on the connections formed by Thy-1+ neurons. Figure 9 illustrates the effect of a variety of Ca^{2+} current blockers on glutamatergic synaptic transmission. It can be seen that evoked EPSCs were completely blocked by Cd^{2+} (50 µM) or Gd^{3+} (10 µM). However, nifedipine, an L-type Ca^{2+} channel antagonist, not only lacked a blocking action, but even increased the amplitudes of evoked EPSCs (Fig. 9*D*). ω-CgTx-GVIA caused a partial block, with a substantial amount of the synaptic response (67 ± 29%, $n = 4$) being resistant to a saturating concentration (5 µM). ω-AgaTx-IVA (200 nM) had no effect. Note that spontaneous synaptic activity persisted at antagonist concentrations that caused a complete block of evoked synaptic currents (Fig. 9*B,C*). Figure 12*A* summarizes the action of Ca^{2+} channel blockers on evoked EPSCs.

The results of Figures 10 and 12*A* indicate that the sensitivity of GABAergic synaptic transmission to Ca^{2+} channel blockers was very similar to that of glutamatergic synaptic transmission. Also in case of GABAergic Thy-1+ neurons, the available channel-specific antagonists caused only a partial block of the synaptic response.

In RGNs Ca^{2+} channel blockers have slightly different effects on transmitter release and somatic Ca^{2+} currents

A relatively low sensitivity to the blocking action of channel specific Ca^{2+} current antagonists was found not only in glutamatergic synaptic transmission but also in somatic Ca^{2+} currents of Thy-1+ neurons. All Thy-1+ neurons generated $I_{Ca(V)}$ if activated with voltage steps from −90 to 0 mV. The pharmacological profile of somatic Ca^{2+} currents was studied in a total of 138 Thy-1+ neurons. Figure 11 shows typical current traces from experiments aimed at characterizing the pharmacologically distinct components in compound somatic Ca^{2+} currents. The mean values are summarized in Figure 12*B*. Percentages were calculated from at least four averaged peak amplitudes of $I_{Ca(HVA)}$ during control conditions and during drug application, respectively. To test for a possible interference of the Ca^{2+} current run-up or run-down with the presented data we used bath solution during the usual test period. The relative amplitude of the Ca^{2+} current amounted to 97.0 ± 5.4% of the control ($n = 9$) and was not significantly different from 100%.

As we have previously reported, at least three types of $I_{Ca(HVA)}$ Ca^{2+} currents can be separated on pharmacological grounds (Guenther et al., 1994). Cd^{2+} (50 µM) and Gd^{3+} (10 µM) completely blocked $I_{Ca(HVA)}$ (Figs. 11*A,B*; 12*B*) but spared a consid-

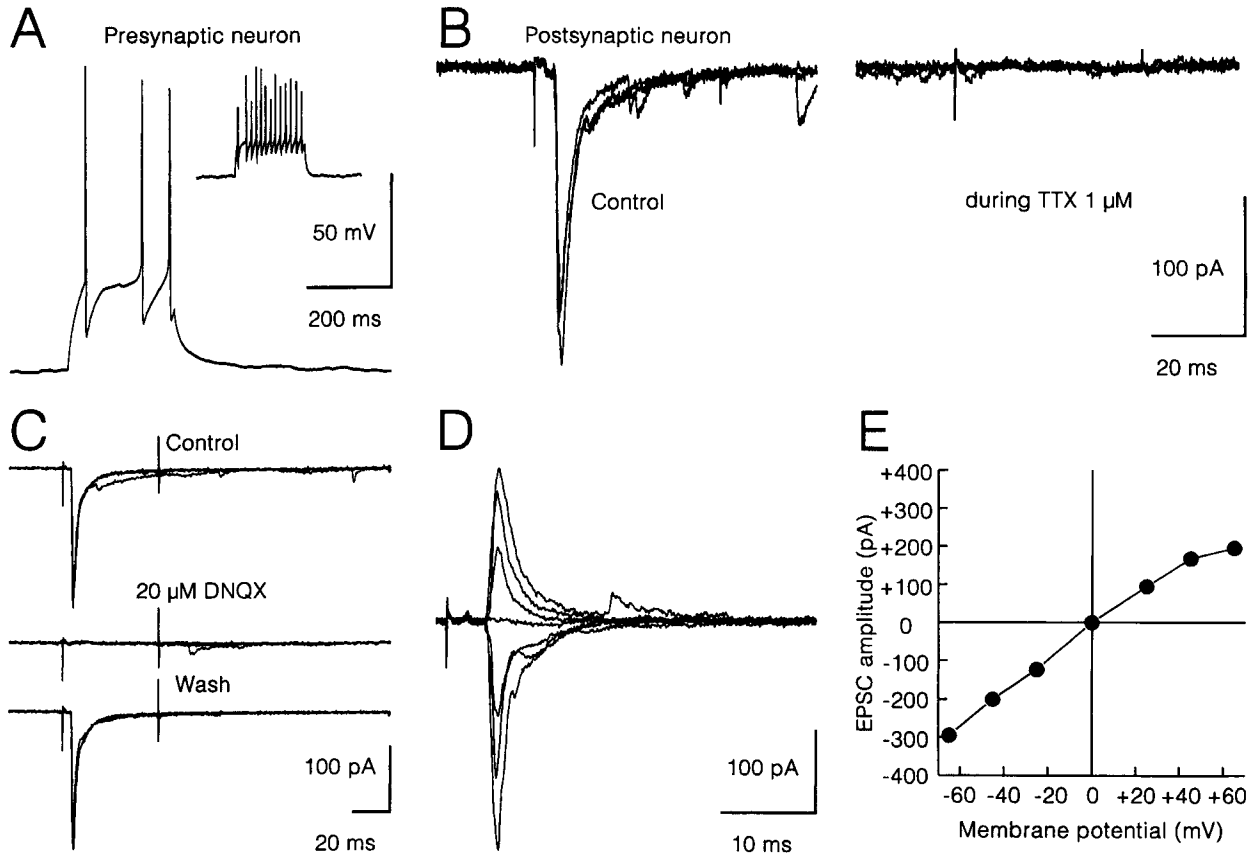

Figure 7. Activation of Glu release from RGNs. *A*, Functional identification of presynaptic strongly labeled Thy-1+ neuron as RGN. Current clamp records show responses to injection of steady depolarizing currents of 100 pA for 250 and 1000 msec (*inset*). Note the absence of spike inactivation, discharge adaptation and slow afterhyperpolarization. This RGN generated a $I_{Na(V)}$ of 12.2 nA (not illustrated). *B*, PSC recorded from a Thy-1–negative neuron responding to depolarization of the cell illustrated in *A*. Block of postsynaptic response by TTX. Records after 13 d *in vitro* at V_h −65 mV. *C*, Identification of glutamatergic EPSCs by complete and reversible block with DNQX. *D* and *E*, Voltage dependence of glutamatergic EPSCs. Superimposed traces (*D*) and current–voltage relationship (*E*) from same cell as *C* after 6 d *in vitro*. Note the roughly linear *I–V* relationship and current reversal at 0 mV. All records in 5 mM $[Ca^{2+}]_o$ and 1 mM $[Mg^{2+}]_o$. Electrodes filled with K-gluconate and CsCl for pre- and postsynaptic recordings, respectively.

erable portion of $I_{Ca(LVA)}$ (Fig. 11*H*). The effect of BAY K8644 on $I_{Ca(HVA)}$ was bimodal. At low concentrations (0.5 μM) it augmented $I_{Ca(HVA)}$ to 130.5 ± 21.1% of the control (Figs. 11*C*, 12*B*), but it had a blocking action at higher concentrations (>5 μM). A saturating dose of ω-CgTx-GVIA (5 μM) irreversibly blocked $I_{Ca(HVA)}$ to 60.3 ± 12.3% of the control (Figs. 11*E*, 12*B*). ω-AgaTx-IVA (200 nM) had no effect on $I_{Ca(HVA)}$ (Figs. 11*F*, 12*B*). Combined application of three channel-specific Ca^{2+} current blockers reduced somatic currents to 56.8 ± 2.9% (Figs. 11*G*, 12*B*).

In contrast to its effect on synaptic transmission nifedipine (15 μM) reduced somatic $I_{Ca(HVA)}$ but the blocked fraction was rather small (mean current amplitude in the presence of nifedipine 70.2 ± 11.8% of the control) (Figs. 11*D*, 12*B*). This is somewhat in disagreement with previous studies in freshly isolated rat RGNs (Karschin and Lipton, 1989) which suggested that DHP-sensitive L-type channels produced a major part of the compound somatic Ca^{2+} currents. Experiments with nitrendipine rendered similar results as nifedipine.

It should be noted, however, that acutely dissociated RGNs of older animals (P7) generated substantially larger Ca^{2+} currents (mean amplitude 610.0 ± 347.6 pA, $n = 8$), with a significantly higher reduction by DHPs (54.3 ± 7.4% of the control, $n = 6$, $p < 0.01$), as compared to RGNs from the P5 retina. It seems therefore that the relatively high fraction of ω-CgTx-GVIA–sensitive channels may be a characteristic feature of immature RGNs. Postnatal maturation of RGNs could be reflected by preferential incorporation of DHP-sensitive channels. However, this maturation process was obviously not reflected in the pharmacological profile of glutamatergic and GABAergic transmission (compare Fig. 12*A*,*B*).

Discussion

This study presents a new cell culture model for investigation of synaptogenesis *in vitro*. In addition it resolves a long-lasting uncertainty with regard to the transmitter(s) of RGNs and characterizes, for the first time, glutamatergic synapses formed by identified RGNs *in vitro*. We found a close relationship between the degree of Thy-1 expression, on one side, and the size of $I_{Na(V)}$ and capacity for repetitive discharge, on the other side. As a rule, only glutamatergic neurons were strongly labeled with Thy-1, responded with repetitive discharge to steady depolarization and generated $I_{Na(V)}$ larger than 2 nA (Table 1). Thus, in conjunction with functional criteria Thy-1 immunostaining can be used to select putative RGNs in dissociated cell cultures. The following discussion will focus on three main issues: (1) Thy-1 as a marker of RGNs in culture, (2) transmitter(s) of RGNs and the possible role of their intraretinal synaptic connections, and

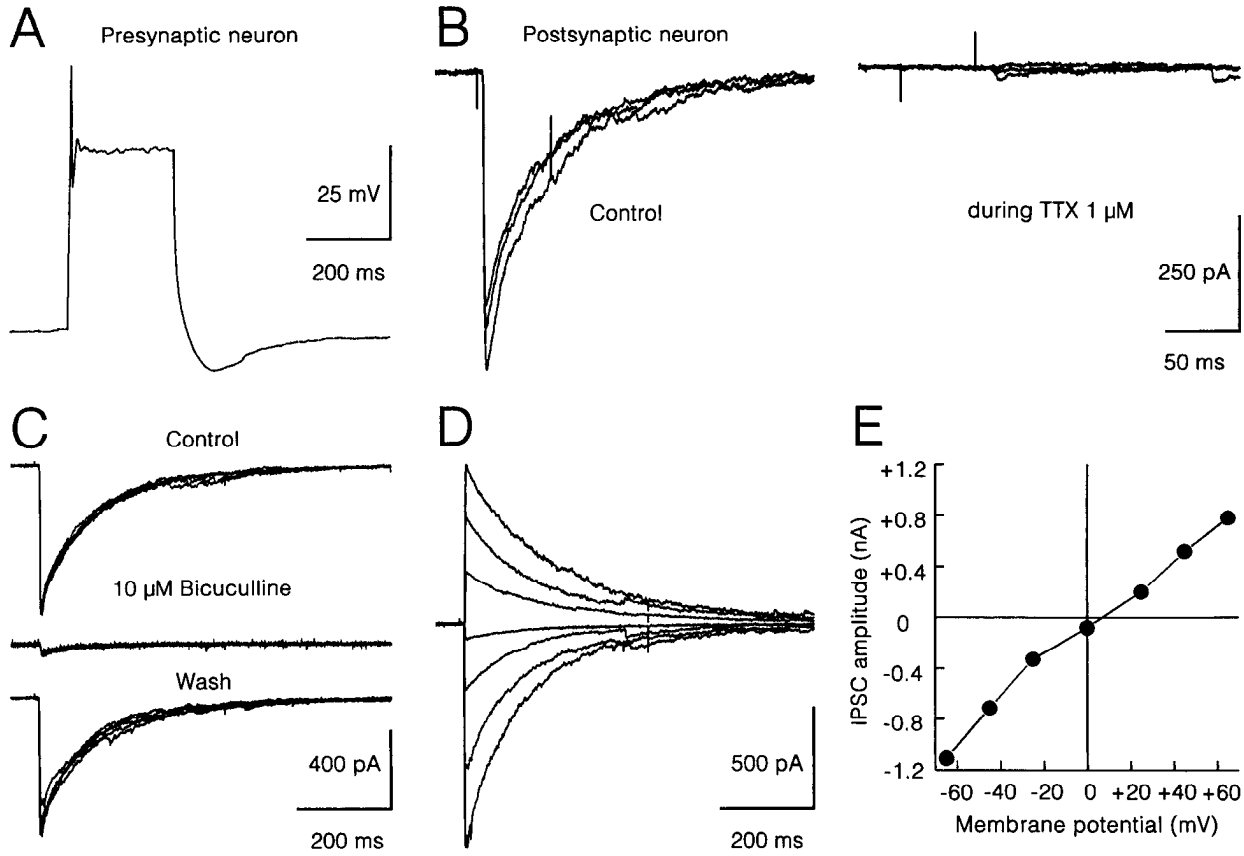

Figure 8. Activation of GABA release from putative displaced amacrine cells. *A*, functional identification of presynaptic neuron as putative amacrine cell. Current-clamp record showing response to injection of steady depolarizing current of 100 pA. Note spike inactivation, pronounced discharge adaptation and slow afterhyperpolarization. This neuron generated a $I_{Na(V)}$ of 0.44 nA (not illustrated). *B*, PSC recorded from a Thy-1– negative neuron responding to depolarization of the cell illustrated in *A*. Block of postsynaptic response by TTX. Records after 13 d *in vitro* at V_h −65 mV. *C–E*, Identification of IPSC by reversible block with bicuculline methiodide, prolonged duration and reversal at about 0 mV (*D, E*). *C–E*, Records after 13 d *in vitro*. Experimental conditions as in Figure 7.

(3) Ca^{2+} channels governing glutamatergic and GABAergic synaptic transmission.

Thy-1 as a marker of RGNs in culture

The observation of two very distinct Thy-1+ neuron populations, that differed not only in their degree of Thy-1 immunostaining and fundamental electrophysiological properties, but also with regard to the released transmitter, raises again the question under which conditions Thy-1 immunostaining could be used for cell identification. The applicability of Thy-1 immunostaining for RGN identification has been subject to doubts because significant labeling was found in the ganglion cell layer after optic nerve section in the postnatal rat (Perry et al., 1984), a lesion that usually causes rapid degeneration of RGNs. Furthermore, double labeling of cultured retinal neurons revealed that not only non-neuronal cells, but at least one neuron class in addition to RGNs could express Thy-1 (Barres et al., 1988). Therefore, we would have possibly refrained from using a mAb against Thy-1 for RGN identification if not the scarcity of vital neuron-specific labeling procedures and the poor survival of GB-labeled RGNs. Fortunately, the pair recording experiments demonstrated that Thy-1 can be used for RGN preselection, if the immunostaining procedure is combined with basic electrophysiological tests.

Thy-1 is a very abundant, developmentally regulated membrane surface glycoprotein with insufficiently characterized role in neuron function (Morris, 1985). We have to consider the possibility that variable neuron pools could sequentially express Thy-1 with the consequence that Thy-1 antibodies may not be selective for any cell type from the rat retina. Furthermore, under the conditions of dissociated cell culture nonphysiological expression of Thy-1 could induce an artificial differentiation process or produce a selective advantage or disadvantage in neuron survival and/or synaptogenesis.

Concerning the first point, as listed above, in neuronal cultures of various origin, only a fraction of all the neurons is labeled with anti-Thy-1. It seems that under appropriate survival conditions larger and more mature neurons may have a higher chance to be Thy-1+ (Liësi et al., 1990). Such observations would support the idea that Thy-1 is primarily a differentiation marker. It is conceivable that the level of Thy-1 expression reflects the developmental state of unmyelinated axons and correlates with the axon length, the size of the innervation field, the firing capacity (present data) and amount of synaptogenesis (see Morris, 1985, for a review). This could explain why in the retina *in vivo* Thy-1 expression is restricted to cells that have an axon and reside in the ganglion cell layer. At no age was a substantial Thy-1 labeling seen in the layers of other cell types (Korenbaum and Grantyn, unpublished observations). Thus, Thy-1 is likely to be expressed solely by RGNs and displaced amacrine cells.

Concerning the second point, that Thy-1 expression may de-

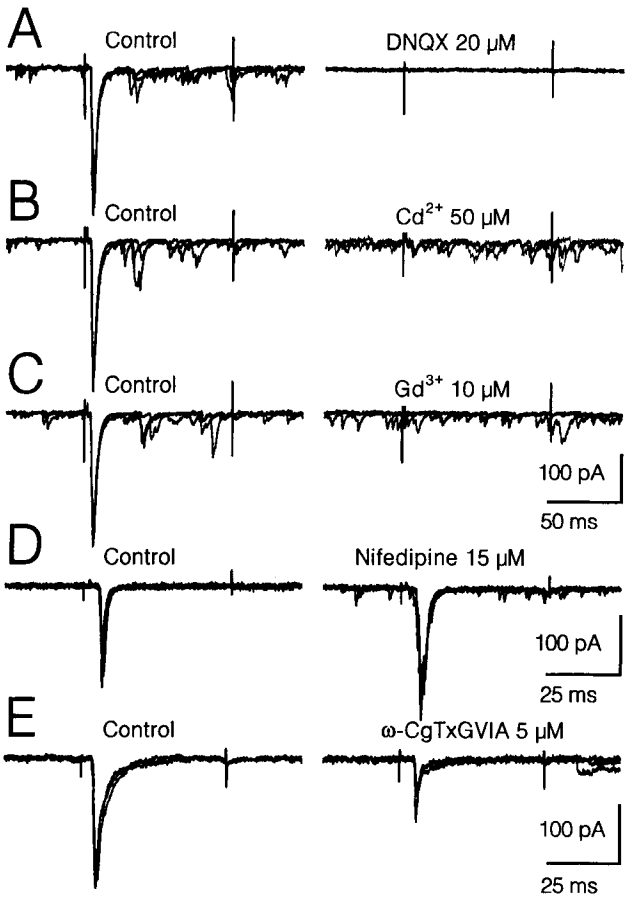

Figure 9. Effect of Glu receptor antagonists and Ca^{2+} channel blockers on glutamatergic EPSCs elicited by stimulation of strongly labeled Thy-1+ RGNs. Records from three different neuron pairs after 9 (*A–C*) and 10 d *in vitro* (*D, E*). To elicit EPSCs, presynaptic RGNs were maintained at V_h −65 mV and step-depolarized to membrane potentials between −20 and +10 mV. Each test was followed by a wash resulting in complete recovery, except the experiment with ω-CgTx-GVIA, where the current reduction remained irreversible. Note that EPSCs could be completely blocked with DNQX (*A*), Cd^{2+} (*B*) and Gd^{3+} (*C*). Nifedipine enhanced synaptic transmission and increased the frequency of spontaneous EPSCs (*D*). ω-CgTx-GVIA caused a partial block of EPSCs (*E*). ω-AgaTx-IVA (200 nM) had no effect (not illustrated). Recording conditions as in Figure 7.

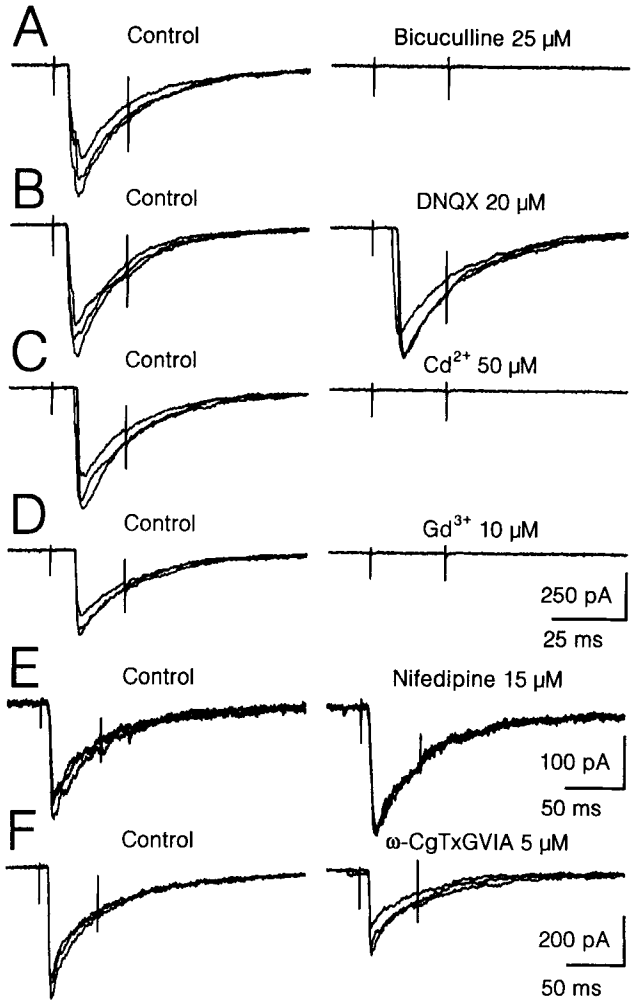

Figure 10. Pharmacological properties of GABAergic IPSCs elicited by stimulation of weakly labeled Thy-1+ neurons. Records from three different neuron pairs after 10 (*A–D*), 10 (*E*), and 14 (*F*) d *in vitro*. To induce IPSCs, presynaptic Thy-1+ neurons were maintained at V_h −65 mV and depolarized to membrane potentials between −20 and 0 mV. Each test was followed by a wash resulting in complete recovery, except the experiment with ω-CgTx-GVIA, where the current reduction remained irreversible. Note that IPSCs were completely blocked by bicuculline methiodide (*A*), but not DNQX (*B*). Low concentrations of Cd^{2+} (*C*) and Gd^{3+} (*D*) completely blocked GABAergic synaptic transmission. Nifedipine slightly increased IPSC amplitudes (*E*), while ω-CgTx-GVIA produced slight IPSC reduction (*F*). Recording conditions as in Figure 7.

pend on environmental factors has been demonstrated in PC12 cells (Richter-Landsberg et al., 1985). No information is currently available on culture conditions which could drive neurons with physiologically low levels of Thy-1 into the direction of increased axonal differentiation and/or Thy-1 expression. But it is not at all excluded that confrontation of GABAergic neurons with the laminin coat of the culture dishes could induce a process of axon differentiation and Thy-1 upregulation that is either entirely lacking *in vivo* or only transiently occurring during physiological development of the rat retina. It has been shown, in fact, that immobilized Thy-1 has the capacity to bind to laminin and fibronectin (Liësi et al., 1990). A more detailed study on better identified amacrine cells in culture is necessary to answer this question.

Taken together, we can conclude that intense Thy-1 immunolabeling in conjunction with repetitive firing over a broad frequency range that closely resembles the discharge behavior of RGNs *in situ* (Mobbs et al., 1992) can be taken as a strong evidence that RGNs survived under our *in vitro* conditions. Identified RGNs *in vitro* may thus be a useful model to study synaptic transmission and synaptogenesis. The identity of weakly labeled GABAergic neurons remains uncertain and has to be clarified.

Transmitter(s) of RGNs and the possible role of intraretinal synapses of RGN axon terminals

Identification of the transmitter substances employed by RGNs for synaptic transmission to their target cells in the retina or the suprachiasmatic nucleus, LGN, pretectum and superior colliculus has been a formidable challenge for many years. Initial attempts by Tebecis (1973) and others were hampered by the lack of suitable receptor blockers. Furthermore, approaches that helped to identify transmitters in other structures, such as retrograde transport of ^{3}H-aspartate, measurement of excitatory

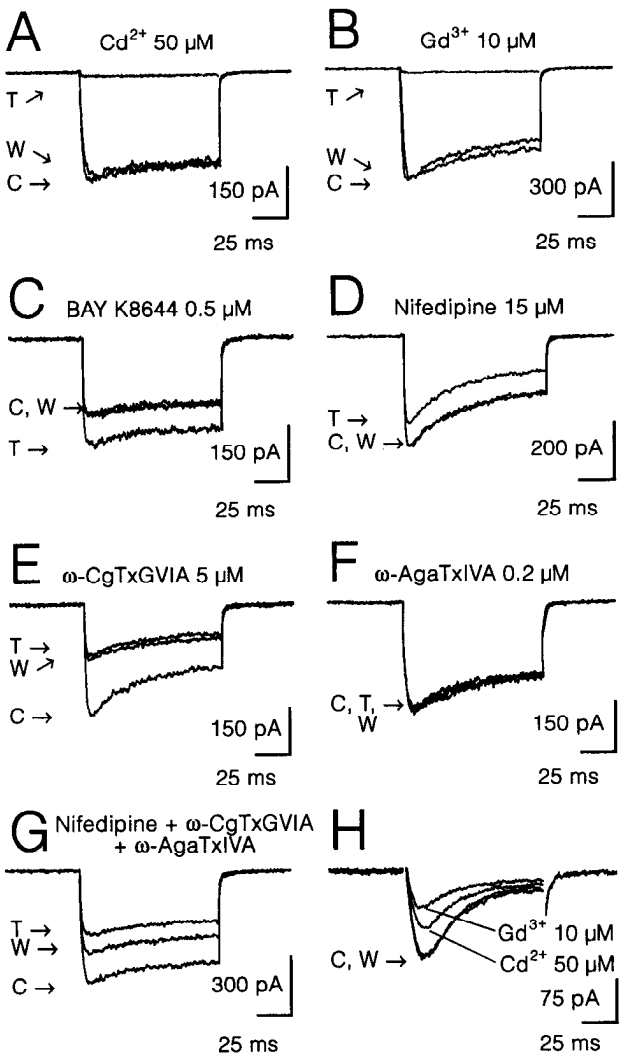

Figure 11. Pharmacological properties of somatic Ca^{2+} currents in RGNs (DIV 1–2). All drugs are indicated above the respective trace. *C*, Control; *T*, test with drug; *W*, trace after washout of drug for at least 1 min. *A–H*, Individual sweeps of compound Ca^{2+} channel currents in 10 mM $BaCl_2$ to activate $I_{Ca(HVA)}$ (voltage steps from −90 mV to 0 mV) or 10 mM $CaCl_2$ to activate $I_{Ca(LVA)}$ (voltage steps from −90 mV to −30 mV), respectively. Linear leak and capacitive currents were subtracted. Small capacitive currents remaining after subtraction were blanked. Note that HVA Ca^{2+} channel currents were completely blocked by 50 µM of Cd^{2+} or 10 µM of Gd^{3+} (*A, B*) while sparing significant portions of $I_{Ca(LVA)}$ (*H*). BAY K8644 increased amplitudes of macroscopic Ca^{2+} channel currents. Nifedipine and ω-CgTx-GVIA induced a partial block of $I_{Ca(HVA)}$ (*C–E*), while ω-AgaTx-IVA had no effect at all on $I_{Ca(HVA)}$ (*F*). At least half of $I_{Ca(HVA)}$ remained during combined application of channel-specific antagonists (*G*).

amino acid content or estimation of Ca^{2+}-dependent release failed to give conclusive results in the rodent retina. Even the available antibodies stained RGNs only weakly, as compared to photoreceptors and bipolar cells (Ehinger et al., 1988; Marc et al., 1990). Nonetheless, already before designing our experiments with pair patch-clamp recording we could regard Glu as a strong candidate for the role of RGN transmitter (Liou et al., 1986; Crunelli et al., 1987; Cahill and Menaker, 1989; Sakurai et al., 1990; Roberts et al., 1991; Hestrin, 1992; Castel et al., 1993). In addition, a Glu containing peptide NAAG (Anderson et al., 1987) and the inhibitory amino acid GABA (Redburn and Madtes, 1986; Yu et al., 1988; Caruso et al., 1989; Lugo-García and Blanco, 1991) were considered to mediate fast synaptic transmission from RGNs in the rodent retina. We concluded that the transmitter released from RGN terminals is Glu because low concentrations of AMPA/kainate receptor blocker DNQX completely abolished the postsynaptic response and the time course of evoked EPSC was strikingly similar to that of other glutamatergic synapses (see Scheggenburger, 1992, for references). The lack of NMDA receptor mediated current components argues against a major role of NAAG.

Now a major open question is whether or not part of the RGN population is inhibitory in nature. Immunostaining of retrogradely or antibody-labeled RGNs with GABA or glutamate decarboxylase, or the presence of high affinity ^{3}H-GABA uptake in ganglion cell layer neurons (Redburn and Madtes, 1986; Yu et al., 1988) has led several authors to the conclusion that a small fraction of RGNs (1–5%) could be GABAergic and inhibitory. The presence of stained axons in the optic nerve fiber layer (Yang et al., 1991) and the demonstration of direct retinal inhibitory synaptic input in the chick optic tectum (Leresche et al., 1986) rendered further support to the hypothesis that a minor population of GABAergic RGNs projects over large distances and activates their targets primarily by disinhibition. Other investigators, however, questioned the existence of an extraretinal GABAergic projection (Grünert and Wässle, 1990) suggesting instead, that all GABAergic neurons in the ganglion cell layer should be attributed to the class of displaced amacrine cells. Considering the limited firing capacity of all GABAergic neurons in culture, we also prefer to think that weakly labeled Thy-1+ neurons *in situ* form only intraretinal connections and belong to the class of displaced amacrine cells.

Although intraretinal axon collaterals of RGNs were repeatedly demonstrated (Dacey, 1985; Lau et al., 1992) it remained unclear whether these fibers formed functional synapses with other retinal neurons and, if so, which cells were the intraretinal targets of RGNs. From recordings *in situ* it became clear that already during the first postnatal week many ganglion cell layer neurons received a glutamatergic synaptic input (Rörig and Grantyn, 1993), although at this age of development bipolar synapses in the inner plexiform layer are not yet developed. We showed now that both putative RGNs and unlabeled multipolar neurons can, in principle, be contacted by glutamatergic Thy-1+ neurons. It would be interesting to further explore the lateral connectivity of neurons in the ganglion cell layer.

Ca^{2+} channels governing glutamate and GABA release from Thy-1+ neurons

Our results provide the following answers to the second question raised in the introduction. (1) Under nonfacilitatory activation conditions (low stimulation frequency, intracellular Ca^{2+} buffering, complete superfusion with salt solutions) Glu release required the participation of at least two different Ca^{2+} channels. About 40% of transmitter release was governed by N-type channels, as indicated by a block with ω-CgTx-GVIA. (2) A major part of the synaptic response was triggered by a class of Ca^{2+} channels that resisted the action of L-type, N-type, and P-type selective antagonists. (3) Glutamatergic and GABAergic Thy-1+ neurons displayed essentially the same pharmacological profile with regard to Ca^{2+} channel antagonists.

With few exceptions (see introductory section), transmitter release from central neurons has been characterized under experimental conditions that did not allow for activation of homoge-

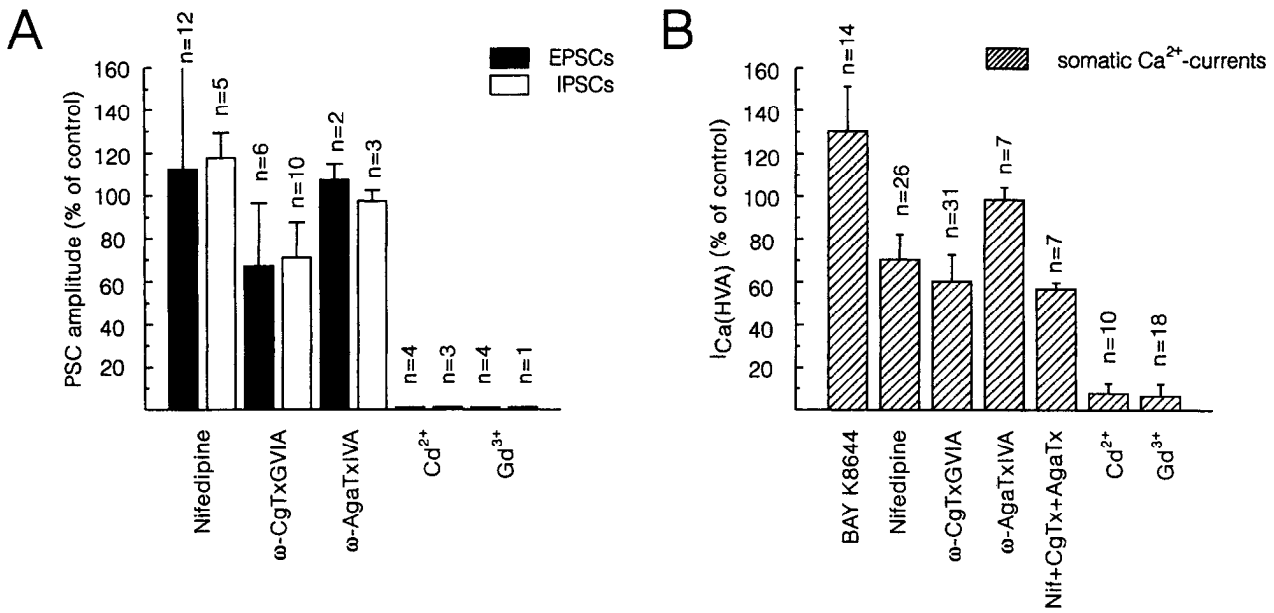

Figure 12. Comparison of the effects of Ca^{2+} channel blockers on Glu and GABA release from synaptically coupled Thy-1+ neurons (*A*) and somatic $I_{Ca(HVA)}$ (*B*). Plots show changes in current amplitudes in percent of the control recorded immediately prior to drug application. In every neuron at least four individual sweeps were averaged for control and test traces. *n*, Number of tested neurons. Note similarity of action on Glu or GABA release and on somatic $I_{Ca(HVA)}$, with the exception of nifedipine which reduced somatic $I_{Ca(HVA)}$ but enhanced synaptic responses.

neous afferent pools. Yet, the stimulation conditions may have considerable consequences for the pharmacological profile of Ca^{2+} dependent transmitter release. For instance, Rane et al. (1987) observed a nifedipine-sensitive substance P release from chick DRG neurons only in case of KCl-induced depolarization. Furthermore, contamination with a GABAergic synaptic input could blur the results of experiments on glutamatergic synaptic transmission, especially in the hippocampal slice preparations where significant differences were found in the toxin sensitivity of excitatory and inhibitory circuits (Potier et al., 1993). Finally, the excessively liberated transmitter itself could alter the pharmacological profile of transmitter release. Krishtal et al. (1989) observed profound changes in the ω-CgTx-GVIA sensitivities of excitatory synaptic transmission in hippocampal cells exposed to Glu. Since the present experiments avoided most of these problems, our estimations of the relative contribution of ω-CgTx-GVIA–sensitive and –insensitive Ca^{2+} channels to Glu release may be regarded as sufficiently reliable.

By now it seems already clear that no strict correspondence exists between the type of transmitter substance(s) and the type of channel(s) involved in synaptic release. In some neurons Glu release is largely dependent on L-channels (Heidelberger and Matthews, 1992; Tachibana et al., 1993) or P-channels (Castillo et al., 1994; Regehr and Mintz, 1994), while in others release is highly resistant to the toxins (Turner et al., 1993) or to DHPs (Castillo et al., 1994). Cholinergic synapses, too, may either be governed by P-channels (Uchitel et al., 1992) or by N-channels (Stanley and Atrakchi, 1990). An age-dependent preferential control of acetylcholine release by L- or N-type channels has also been reported (Gray et al., 1992). These results underline the necessity of studies using selected neuron populations under defined environmental conditions. With regard to the toxin- and DHP-resistant component of Glu release one can only speculate that the responsible Ca^{2+} channel may be one of the recently described Q- (Randall et al., 1993) or R-type (Ellinor et al., 1993) Ca^{2+} channels. The toxin- and DHP-resistant Ca^{2+} channel of RGNs deserves further investigation when new pharmacological tools become available.

Most publications agree in that DHP-sensitive L-type channels play only a minor role in synaptic transmission. An exception from this rule is the goldfish bipolar cell. In some cells DHP-induced protein kinase C stimulation could lead to a Ca^{2+} channel upregulation (Fossier et al., 1992). This may result in enhanced transmitter release (O'Regan et al., 1991) and explain our present observations with nifedipine. Since we did not attempt at clarifying the mechanisms of the nifedipine-induced enhancement of synaptic transmission, we cannot completely rule out a minor participation of DHP-sensitive Ca^{2+} channels on Glu or GABA release from Thy-1+ neurons.

A participation of LVA Ca^{2+} channels in synaptic transmission has not been conclusively demonstrated, although such a possibility may exist in peripheral neurons (Seabrook and Adams, 1989). Our results confirm previous observations made with excitatory synaptic connections between cultured thalamic neurons (Pfrieger et al., 1992) in showing that the currents prevailing after complete block of somatic HVA current components were not sufficient to trigger Glu release.

References

Anderson KJ, Borja MA, Cotman CW, Moffett JR, Namboodiri MAA, Neale JH (1987) *N*-Acetylaspartylglutamate identified in the rat retinal ganglion cells and their projections in the brain. Brain Res 411: 172–177.

Balkema GW, Pinto LH (1982) Electrophysiology of retinal ganglion cells in the mouse: a study of a normally pigmented mouse and a congenic hypopigmentation mutant, pearl. J Neurophysiol 48:968–980.

Barres BA, Silverstein BE, Corey DP, Chun LLY (1988) Immunological, morphological, and electrophysiological variation among retinal ganglion cells purified by panning. Neuron 1:791–803.

Brecha N, Johnson D, Bolz J, Sharma S, Parnavelas JG, Lieberman AR

(1987) Substance P–immunoreactive retinal ganglion cells and their central axon terminals in the rabbit. Nature 327:155–158.
Cahill GM, Menaker M (1989) Responses of suprachiasmatic nucleus to retinohypothalamic tract volleys in a slice preparation of the mouse hypothalamus. Brain Res 479:65–75.
Caruso DM, Owczarzak MT, Goebel DJ, Hazlett JC, Pourcho RG (1989) GABA-immunoreactivity in ganglion cells of the rat retina. Brain Res 476:129–134.
Castel M, Belenky M, Cohen S, Ottersen OP, Storm-Mathisen J (1993) Glutamate-like immunoreactivity in retinal terminals of the mouse suprachiasmatic nucleus. Eur J Neurosci 5:368–381.
Castillo PE, Weisskopf MG, Nicoll RA (1994) The role of Ca^{2+} channels in hippocampal mossy fiber synaptic transmission and long-term potentiation. Neuron 12:261–269.
Crunelli V, Kelly JS, Leresche N, Pirchio M (1987) On the excitatory post-synaptic potential evoked by stimulation of the optic tract in the rat lateral geniculate nucleus. J Physiol (Lond) 384:603–618.
Dacey DM (1985) Wide-spreading terminal axons in the inner plexiform layer of the cat's retina: evidence for intrinsic axon collaterals of ganglion cells. J Comp Neurol 242:247–262.
Dacey DM (1990) The dopaminergic amacrine cell. J Comp Neurol 301:461–489.
Ehinger B, Ottersen OP, Storm-Mathisen J, Dowling JE (1988) Bipolar cells in the turtle retina are strongly immunoreactive for glutamate. Proc Natl Acad Sci USA 85:8321–8325.
Ellinor PT, Zhang J-F, Randall AD, Zhou M, Schwarz TL, Tsien RW, Horne WA (1993) Functional expression of a rapidly inactivating neuronal calcium channel. Nature 363:455–458.
Fossier P, Baux G, Trudeau L-E, Tauc L (1992) Pre- and postsynaptic actions of nifedipine at an identified cholinergic central synapse of *Aplysia*. Pfluegers Arch 422:193–197.
Gleason E, Borges S, Wilson M (1993) Synaptic transmission between pairs of retinal amacrine cells in culture. J Neurosci 13:2359–2370.
Grantyn R, Korenbaum E (1992) Easy identification of dissociated rat retinal ganglion cells by a size criterion. In: Practical electrophysiological methods: a guide for *in vitro* studies in vertebrate neurobiology (Kettenmann H, Grantyn R, eds), pp 84–87. New York: Wiley-Liss.
Grantyn R, Grantyn A, Schierwagen A (1983) Passive membrane properties, afterpotentials and repetitive firing of superior colliculus neurons studied in the anesthetized cat. Exp Brain Res 50:377–391.
Gray DB, Brusés JL, Pilar GR (1992) Developmental switch in the pharmacology of Ca^{2+} channels coupled to acetylcholine release. Neuron 8:715–724.
Grünert U, Wässle H (1990) GABA-like immunoreactivity in the macaque monkey retina: a light and electron microscopic study. J Comp Neurol 297:509–524.
Guenther E, Rothe T, Taschenberger H, Grantyn R (1994) Separation of calcium currents in retinal ganglion cells from postnatal rat. Brain Res 633:223–235.
Heidelberger R, Matthews G (1992) Calcium influx and calcium current in single synaptic terminals of goldfish retinal bipolar neurons. J Physiol (Lond) 447:235–256.
Hestrin S (1992) Developmental regulation of NMDA receptor-mediated synaptic currents at a central synapse. Nature 357:686–689.
Hinds JW, Hinds PL (1983) Development of retinal amacrine cells in the mouse embryo: evidence for two modes of formation. J Comp Neurol 213:1–23.
Huettner JE, Baughman RW (1988) The pharmacology of synapses formed by identified corticocollicular neurons in primary cultures of rat visual cortex. J Neurosci 8:160–175.
Johnson JE, Barde Y-A, Schwab M, Thoenen H (1986) Brain-derived neurotrophic factor supports the survival of cultured rat retinal ganglion cells. J Neurosci 6:3031–3038.
Karschin A, Lipton SA (1989) Calcium channels in solitary retinal ganglion cells from post-natal rat. J Physiol (Lond) 418:379–396.
Kraszewski K, Grantyn R (1992) Unitary, quantal and miniature GABA-activated synaptic chloride currents in cultured neurons from the rat superior colliculus. Neuroscience 47:555–570.
Krishtal OA, Petrov AV, Smirnov SV, Nowycky MC (1989) Hippocampal synaptic plasticity induced by excitatory amino acids includes changes in sensitivity to the calcium channel blocker, omega-conotoxin. Neurosci Lett 102:197–204.
Kuffler SW (1953) Discharge patterns and functional organization of mammalian retina. J Neurophysiol 16:37–68.
Lankheet MJM, Molenaar J, van de Grind WA (1989) Frequency transfer properties of the spike generating mechanism of cat retinal ganglion cells. Vision Res 29:1649–1661.
Lau KC, So K-F, Tay D (1992) Postnatal development of type I retinal ganglion cells in hamsters: a Lucifer yellow study. J Comp Neurol 315:375–381.
Leresche N, Hardy O, Audinat E, Jassik-Gerschenfeld D (1986) Synaptic organization of inhibitory circuits in the pigeon's optic tectum. Brain Res 365:383–387.
Liësi P, Salonen E-M, Dahl D, Vaheri A, Richards S-J (1990) Thy-1 is a neuronal and glial surface antigen which interacts with matrix proteins and plasminogen activator. Exp Brain Res 79:642–650.
Liou SY, Shibata S, Iwasaki K, Ueki S (1986) Optic nerve stimulation-induced increase of release of ^{3}H-glutamate and ^{3}H-aspartate but not ^{3}H-GABA from the suprachiasmatic nucleus in slices of rat hypothalamus. Brain Res Bull 16:527–531.
Lugo-García N, Blanco RE (1991) Localization of GAD- and GABA-like immunoreactivity in ground squirrel retina: retrograde labeling demonstrates GAD-positive ganglion cells. Brain Res 564:19–26.
Marc RE, Liu W-LS, Kalloniatis M, Raiguel SF, Van Haesendonck E (1990) Patterns of glutamate immunoreactivity in the goldfish retina. J Neurosci 10:4006–4034.
Matthews G, Ayoub GS, Heidelberger R (1994) Presynaptic inhibition by GABA is mediated via two distinct GABA receptors with novel pharmacology. J Neurosci 14:1079–1090.
Mobbs P, Everett K, Cook A (1992) Signal shaping by voltage-gated currents in retinal ganglion cells. Brain Res 574:217–223.
Morris R (1985) Thy-1 in developing nervous tissue. Dev Neurosci 7:133–160.
O'Regan MH, Kocsis JD, Waxman SG (1991) Nimodipine and nifedipine enhance transmission at the Schaffer collateral CA1 pyramidal neuron synapse. Exp Brain Res 84:224–228.
Perry VH, Morris RJ, Raisman G (1984) Is Thy-1 expressed only by ganglion cells and their axons in the retina and optic nerve? J Neurocytol 13:809–824.
Pfrieger FW, Veselovsky NS, Gottmann K, Lux HD (1992) Pharmacological characterization of calcium currents and synaptic transmission between thalamic neurons *in vitro*. J Neurosci 12:4347–4357.
Potier B, Dutar P, Lamour Y (1993) Different effects of omega-conotoxin GVIA at excitatory and inhibitory synapses in rat CA1 hippocampal neurons. Brain Res 616:236–241.
Randall AD, Wendland B, Schweizer F, Miljanich G, Adams ME, Tsien RW (1993) Five pharmacologically distinct high voltage-activated Ca^{2+} channels in cerebellar granule cells. Soc Neurosci Abstr 19: 1478.
Rane SG, Holz IV GG, Dunlap K (1987) Dihydropyridine inhibition of neuronal calcium current and substance P release. Pfluegers Arch 409:361–366.
Redburn DA, Madtes P, Jr (1986) Postnatal development of ^{3}H-GABA-accumulating cells in rabbit retina. J Comp Neurol 243:41–57.
Regehr WG, Mintz IM (1994) Participation of multiple calcium channel types in transmission at single climbing fiber to Purkinje cell synapses. Neuron 12:605–613.
Richter-Landsberg C, Greene LA, Shelanski ML (1985) Cell surface Thy-1–cross-reactive glycoprotein in cultured PC12 cells: modulation by nerve growth factor and association with the cytoskeleton. J Neurosci 2:468–476.
Roberts WA, Eaton SA, Salt TE (1991) Excitatory amino acid receptors mediate synaptic responses to visual stimuli in superior colliculus neurones of the rat. Neurosci Lett 129:161–164.
Rodríguez-Tébar A, Jeffrey PL, Thoenen H, Barde Y-A (1989) The survival of chick retinal ganglion cells in response to brain-derived neurotrophic factor depends on their embryonic age. Dev Biol 136: 296–303.
Rörig B, Grantyn R (1993) Glutamatergic and GABAergic synaptic currents in ganglion cells from isolated retinae of pigmented rats during postnatal development. Dev Brain Res 74:98–110.
Rothe T, Bigl V, Grantyn R (1994) Potentiating and depressant effects of metabotropic glutamate receptor agonists on high-voltage-activated calcium currents in cultured retinal ganglion neurons from postnatal mice. Pfluegers Arch 426:161–170.
Sakurai T, Miyamoto T, Okada Y (1990) Reduction of glutamate content in rat superior colliculus after retino-tectal denervation. Neurosci Lett 109:299–303.
Schneggenburger R, López-Barneo J, Konnerth A (1992) Excitatory

and inhibitory synaptic currents and receptors in rat medial septal neurones. J Physiol (Lond) 445:261–276.
Seabrook GR, Adams DJ (1989) Inhibition of neurally-evoked transmitter release by calcium channel antagonists in rat parasympathetic ganglia. Br J Pharmacol 97:1125–1136.
Sillito AM, Murphy PC, Salt TE, Moody CI (1990) Dependence of retinogeniculate transmission in cat on NMDA receptors. J Neurophysiol 63:347–355.
Stanley EF (1993) Single calcium channels and acetylcholine release at a presynaptic nerve terminal. Neuron 11:1007–1011.
Stanley EF, Atrakchi AH (1990) Calcium currents recorded from a vertebrate presynaptic nerve terminal are resistant to the dihydropyridine nifedipine. Proc Natl Acad Sci USA 87:9683–9687.
Stone C, Pinto LH (1993) Response properties of ganglion cells in the isolated mouse retina. Visual Neurosci 10:31–39.
Tachibana M, Okada T, Arimura T, Kobayashi K, Piccolino M (1993) Dihydropyridine-sensitive calcium current mediates neurotransmitter release from bipolar cells of the goldfish retina. J Neurosci 13:2898–2909.
Takahashi N, Cummins D, Caprioli J (1991) Rat retinal ganglion cells in culture. Eye Res 53:565–572.
Taschenberger H, Grantyn R (1993) Two types of spontaneous excitatory synaptic currents in cultures from the postnatal rat retina. In: Proceedings of the 21th Göttingen Neurobiology Conference, Gene–brain–behaviour (Elsner N, Heisenberg M, eds), pp 407. Stuttgart: Thieme.
Tebecis AK (1973) Studies on the identity of the optic nerve transmitter. Brain Res 63:31–42.
Turner TJ, Adams ME, Dunlap K (1993) Multiple Ca^{2+} channel types coexist to regulate synaptosomal neurotransmitter release. Proc Natl Acad Sci USA 90:9518–9522.
Uchitel OD, Protti DA, Sanchez V, Cherksey BD, Sugimori M, Llinás R (1992) P-Type voltage-dependent calcium channel mediates presynaptic calcium influx and transmitter release in mammalian synapses. Proc Natl Acad Sci USA 89:3330–3333.
Yang C-Y, Lukasiewicz P, Maguire G, Werblin FS, Yazulla S (1991) Amacrine cells in the tiger salamander retina: morphology, physiology, and neurotransmitter identification. J Comp Neurol 312:19–32.
Yu BC-Y, Watt CB, Lam DMK, Fry KR (1988) GABAergic ganglion cells in the rabbit retina. Brain Res 439:376–382.
Yu C, Lin P-X, Fitzgerald S, Nelson P (1992) Heterogeneous calcium currents and transmitter release in cultured mouse spinal cord and dorsal root ganglion neurons. J Neurophysiol 67:561–575.